This article has been accepted for inclusion in a future issue of this journal. Content is final as presented, with the exception of pagination.

Fat-Tree-Based Optical Interconnection Networks Under Crosstalk Noise Constraint

Mahdi Nikdast, *Student Member, IEEE*, Jiang Xu, *Member, IEEE*, Luan H. K. Duong, Xiaowen Wu, *Student Member, IEEE*, Zhehui Wang, *Student Member, IEEE*, Xuan Wang, *Student Member, IEEE*, and Zhe Wang

***Abstract*— Optical networks-on-chip (ONoCs) have shown the potential to be substituted for electronic networks-on-chip (NoCs) to bring substantially higher bandwidth and more efficient power consumption in both on- and off-chip communication. However, basic optical devices, which are the key components in constructing ONoCs, experience inevitable crosstalk noise and power loss; the crosstalk noise from the basic devices accumulates in large-scale ONoCs and considerably hurts the signal-to-noise ratio (SNR) as well as restricts the network scalability. For the first time, this paper presents a formal system-level analytical approach to analyze the worst-case crosstalk noise and SNR in arbitrary fat-tree-based ONoCs. The analyses are performed hierarchically at the basic optical device level, then at the optical router level, and finally at the network level. A general 4 × 4 optical router model is considered to enable the proposed method to be adaptable to fat-tree-based ONoCs using an arbitrary 4 × 4 optical router. Utilizing the proposed general router model, the worst-case SNR link candidates in the network are determined. Moreover, we apply the proposed analyses to a case study of fat-tree-based ONoCs using an optical turnaround router (OTAR). Quantitative simulation results indicate low values of SNR and scalability constraints in large scale fat-tree-based ONoCs, which is due to the high power of crosstalk noise and power loss. For instance, in fat-tree-based ONoCs using the OTAR, when the injection laser power equals 0 dBm, the crosstalk noise power is higher than the signal power when the number of processor cores exceeds 128; when it is equal to 256, the signal power, crosstalk noise power, and SNR are −17.3, −11.9, and −5.5 dB, respectively.**

***Index Terms*— Optical crosstalk noise, optical interconnection networks, optical losses, signal-to-noise ratio (SNR), fat-tree-based optical networks-on-chip (ONoCs).**

I. Introduction

EVER-INCREASING demand for higher computing performance, on one hand, and the rapid advance of the semiconductor technology roadmap into the deeper Submicron domain, on the other, have driven the trend of integrating a large number of processing cores on a single die. To satisfy the performance requirements needed in the multicore era, networks-on-chip (NoCs) have been proposed to outperform interconnects in the traditional interconnection networks [1]. However, as new applications demand integrating an even larger number of processing cores on a chip, the metallic interconnects in NoCs cannot keep pace with such developments because of their inability to meet the required bandwidth and latency while efficiently consuming power. Furthermore, studies have shown the critical role of efficient interconnects in future multiprocessor systems-on-chip (MPSoCs) [2]. Recent advances in silicon-based nanotechnology enable the introduction of optical networks-on-chip (ONoCs) in MPSoCs to offer ultrahigh bandwidth, lower power dissipation, and latency.

Optical NoCs are based on on-chip optical interconnects and routers [3]. Optical routers, which play a fundamental role in on-chip communication in ONoCs, are constructed using basic photonic devices such as microresonators (MRs) and waveguide crossings. The number of basic photonic devices in constructing ONoCs scales with the network size. These devices, however, suffer from intrinsic, inevitable crosstalk noise, and power loss due to their imperfection. The intrachannel homodyne crosstalk, when the optical crosstalk noise is at the same wavelength as the transmitted signal, is of critical concern because it cannot be removed by filtering [4], [5]. Within the homodyne crosstalk noise, incoherent crosstalk, whose phase is uncorrelated with the optical signal, introduces quick power fluctuations, whereas coherent crosstalk, whose phase is correlated with the optical signal, varies the optical power of the optical signal [6]–[8]. In this paper, we consider incoherent crosstalk noise, and, for convenience, we will refer to it as crosstalk noise in the rest of this paper. In large-scale ONoCs, the crosstalk noise from photonic devices accumulates on the optical signal, causes power fluctuations at the receiver and consequently weakens the signal-to-noise ratio (SNR) and restricts the network scalability. Hence, to guarantee faultless and reliable on-chip optical communication, it is vital to be able to analyze the worst-case crosstalk noise and SNR in ONoCs.

The fat-tree topology resembles a complete binary tree, in which more than one interconnect exists between a node and its parent, resulting in a high throughput that makes it a promising routing network for multiprocessor systems. Fat-tree-based Optical NoCs have been proposed to take advantage of the fat-tree topology to provide better throughput, power efficiency, and signal latency in ONoCs [9]. The traditional fat-tree network, also known as H-tree, has many waveguide crossings, and as the

Manuscript received May 7, 2013; revised November 8, 2013; accepted December 29, 2013. This work was supported by Grant GRF620911, Grant GRF620512, and Grant DAG11EG05S.

The authors are with the Department of Electronic and Computer Engineering, Hong Kong University of Science and Technology, Hong Kong (e-mail: mnikdast@ust.hk; jiang.xu@ust.hk; hklduong@ust.hk; wxxaf@ust.hk; zhehui@ust.hk; eexwang@ust.hk; zhe.wang@ust.hk).

Color versions of one or more of the figures in this paper are available online at http://ieeexplore.ieee.org.

Digital Object Identifier 10.1109/TVLSI.2014.2300534

1063-8210 © 2014 IEEE. Personal use is permitted, but republication/redistribution requires IEEE permission.
See http://www.ieee.org/publications_standards/publications/rights/index.html for more information.

This article has been accepted for inclusion in a future issue of this journal. Content is final as presented, with the exception of pagination.

network scales, the number of crossings increases, and accordingly, the power consumption greatly rises. To overcome such issues, an optimized floorplan of fat-tree-based ONoCs, considered in this paper, was proposed in [10]. Compared with the traditionally used H-tree floorplan, more than 87% of crossings are reduced in the optimized floorplan. Furthermore, the average interconnect length and traversal distance as well as the maximum interconnect length are efficiently reduced. As a result, optimized fat-tree-based ONoCs offer better power consumption and throughput.

Considering the formal analytical method developed in [11], the proposed analytical models at the basic device level can be used in any topology, while the optical router level analyses are based on a general 5×5 optical router model. Besides this, the proposed network level analyses can only be applied to mesh-based ONoCs. The worst-case SNR analysis in a specific ONoC architecture is highly tied to the architectural properties of that ONoC; the worst-case statuses (configurations) of the optical routers in various ONoCs are not the same, necessitating the development of a specific worst-case SNR analytical approach for each ONoC architecture. Therefore, fat-tree-based ONoCs require a unique and novel analytical method at the router and network levels to realize the worst-case SNR analyses in such networks. The novel contribution of this paper is presenting a formal system-level approach to analyze the worst-case SNR and crosstalk noise in optimized fat-tree-based ONoCs. Following the same bottom-up strategy as in [11], we hierarchically start with analyzing the basic photonic devices, continue with the optical router level analytical models, and finally propose the worst-case crosstalk noise and SNR models at the network level.

A general 4×4 optical router model, which can be applied to any 4×4 optical router, is considered. The general optical router model helps the proposed analyses easily adapt to fat-tree-based ONoCs using an arbitrary 4×4 optical router. Utilizing the proposed general router model and the basic devices analyses, the worst-case SNR of different longest optical links are analyzed and compared to find the worst-case SNR candidates in fat-tree-based ONoCs. We present the quantitative simulations of the worst-case SNR candidates to indicate the SNR and crosstalk noise variations under different numbers of processor cores in fat-tree-based ONoCs. A case study of fat-tree-based ONoCs using an optical turnaround router (OTAR), as proposed in [9], is presented. The considered fat-tree-based ONoC is a hierarchical, multistage network in which payload data and network control data are both being transmitted on the same optical network. Moreover, circuit switching and packet switching are used respectively while transmitting the payload and network control data. Dynamic variations of basic photonic devices due to the laser and thermal noise as well as fabrication variations can affect the SNR analyses; nevertheless, they are not considered in this paper. We assume the use of an on-chip vertical cavity surface emitting laser (VCSEL) as the laser source.

The rest of this paper is organized as follows. Section II summarizes some of the related works discussing the crosstalk noise issue at the device and network levels in ONoCs. Section III describes the basic photonic devices' analytical models and the general 4×4 optical router model. In Section IV, the analytical models at the device and router levels are utilized to analyze and determine the worst-case SNR link candidates in fat-tree-based ONoCs. Moreover, the quantitative simulations of the worst-case SNR candidates are described in this section. We apply the proposed analyses to a case study of fat-tree-based ONoCs using an OTAR in Section V. Section VI concludes our paper.

II. Summary of Related Works

Some efforts have been made to alleviate the crosstalk noise and power loss issues in basic photonic devices. Zhang *et al.* [12] demonstrated a waveguide crossing for Submicron silicon waveguides with an average insertion loss of 0.18 ± 0.03 dB and crosstalk of 41 ± 2 dB. Tsarev *et al.* [13] introduced an efficient silicon wire waveguide crossing by means of vertical coupling of tapered Si wire with an upper polymer wide strip waveguide through a silica buffer to provide 98% efficiency for through pass and 99.9% efficiency for cross pass, as well as a negligible back reflection of -50 dB and crosstalk noise of -70 dB. Ding *et al.* [14] proposed a waveguide crossing mechanism based on impedance matched metamaterials with large absolute values of negative refractive indexes and obtained a very low insertion loss and crosstalk noise of -0.04 and -40 dB, respectively. Xia *et al.* [15] demonstrated compact, photonic-wire-based coupled resonator optical waveguide structures, including up to 16 racetrack resonators on a silicon-on-insulator (SOI) substrate and indicated a drop port loss of less than 3 dB. In [16], the same group presented ultracompact fifth-order ring resonator optical filters based on Submicron silicon photonic wires. Li *et al.* [17] designed and fabricated a compact third-order coupled-resonator filter on the SOI platform with focused application for on-chip optical interconnects and obtained a drop port loss of less than 0.5 dB, an in-band throughput-port extinction of 12 dB and an out-of-band drop rejection of 18 dB.

In addition to the aforementioned works, there are a number of research works exploring the crosstalk noise issue in on-chip interconnection networks at the network level. Xie *et al.* [18] analyzed the worst-case crosstalk noise and SNR in mesh-based ONoCs using an optimized optical crossbar router and introduced a novel compact optical router, called Crux, to outperform the SNR in ONoCs. In the same work, it was proved that the worst-case SNR link in mesh-based ONoCs is not the longest optical link, which suffers from the maximum power loss in the network. Analytical, formal methods to analyze the worst-case signal power, crosstalk noise power, and SNR in arbitrary mesh-based and folded-torus-based ONoCs were proposed in [11] and [19]. Chan *et al.* [20] described a methodology for modeling and analyzing optical interconnection networks at both the physical- and system-level. In [21], Ding *et al.* presented GLOW, a hybrid global router, to provide low power optoelectronic interconnect synthesis while considering thermal reliability and various physical design constraints such as optical power, delay and signal quality. Lin *et al.* [22] developed an analytical model to

This article has been accepted for inclusion in a future issue of this journal. Content is final as presented, with the exception of pagination.

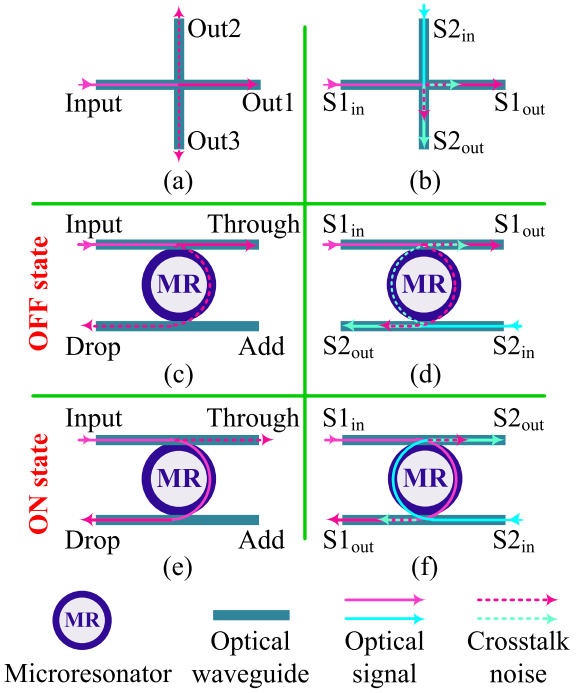

Fig. 1. (a) and (b) Waveguide crossing. (c) and (d) Parallel switching element in the OFF state, and (e) and (f) in the ON state.

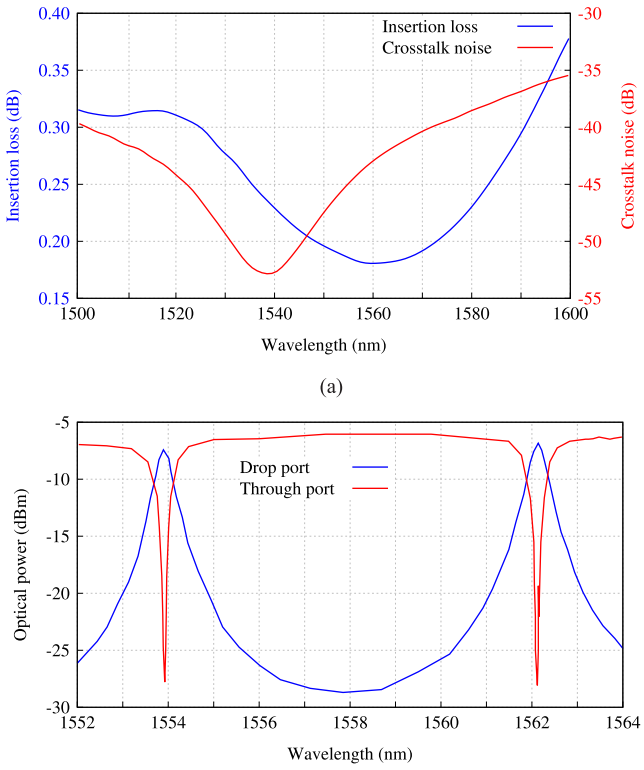

Fig. 2. Power loss and crosstalk noise in a waveguide crossing and an active parallel switching element. (a) Waveguide crossing [23]. (b) Active parallel switching element [24].

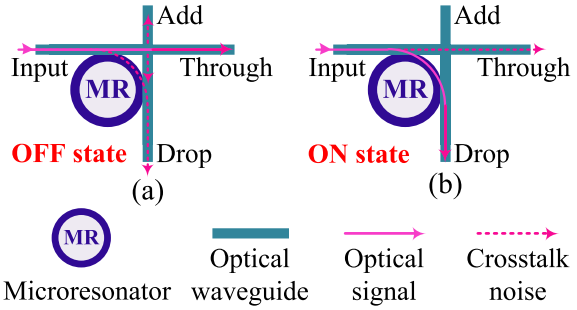

Fig. 3. Crossing switching element in (a) OFF state and (b) ON state.

characterize the crosstalk noise level in a microring-based optical interconnection network.

III. Crosstalk Noise in Basic Photonic Devices and Optical Routers

Basic photonic devices are widely employed to construct optical routers and ONoCs. Among such devices, waveguides and microresonators form different types of optical elements, including waveguide crossings, waveguide bendings, and basic optical switching elements (BOSEs). The costly multilayer fabrication process and the need for compact optical routers necessitate integrating these devices on a single silicon layer. As a result, due to the mode coupling in the optical signals, such devices transmit optical signals while imposing power loss and crosstalk noise. For instance, in a waveguide crossing, which consists of two orthogonal waveguides [see Fig. 1(a)], optical modes propagate with insertion loss from the input port to the output port out1, whereas a portion of the optical power propagates to the other output ports, out2 and out3. Fig. 2(a) shows the insertion loss and crosstalk noise in a typical waveguide crossing as a function of the wavelength [23]. As can be seen from the figure, the minimum insertion loss of 0.17 dB is roughly at the wavelength of 1560 nm, whereas at the same wavelength the crosstalk noise is almost equal to -43 dB.

Using waveguides and microresonators, two types of 1×2 basic optical switching elements can be designed, including parallel switching elements (PSEs), Fig. 1(c)–(f), and crossing switching elements (CSEs), Fig. 3. BOSEs can use either an active or passive microresonator-based switching. In the active microresonator-based switching, considered in this paper, MRs can be switched on by applying an electrical voltage to the p-n contacts surrounding the ring. Considering the passive microresonator-based switching, the equivalence (difference) between the resonance frequency of the MR and the modulation frequency of the optical signal determines the ON (the OFF) state of the MR. When an optical signal enters the input port of a PSE in the OFF state, it propagates with some passing power loss from the input port to the through port, while a portion of the optical power goes to the drop port as crosstalk noise. However, in the ON state, the optical signal turns from the input port to the drop port with some power loss, while creating crosstalk noise on the through port. Fig. 2(b) shows the function of an active PSE, in which the 3 dB pass band is measured to be roughly 0.4 nm [24]. According to this figure, when the MR is turned on, for example, at the wavelength of 1554 nm, the optical power at

This article has been accepted for inclusion in a future issue of this journal. Content is final as presented, with the exception of pagination.

TABLE I
NOTATIONS FOR POWER LOSSES AND CROSSTALK COEFFICIENTS

Parameter	Notation
Crossing loss	L_c
Propagation loss	L_p
Power loss per CSE in the OFF state	L_{c0}
Power loss per CSE in the ON state	L_{c1}
Bending loss	L_b
Passing loss per PSE in the OFF state	L_{p0}
Drop loss per PSE in the ON state	L_{p1}
Crossing's crosstalk coefficient	X_c
Crosstalk coefficient per PSE in the OFF state	X_{p0}
Crosstalk coefficient per PSE in the ON state	X_{p1}

the drop port is almost -7 dBm, while it is roughly equal to -28 dBm at the through port. By contrast, during the OFF state, the optical power at the drop and through ports are roughly equal to -29 dBm and -6 dBm, respectively.

In this section, we systematically model the power loss and crosstalk noise in waveguide crossings, PSEs and CSEs. Moreover, we present a general 4×4 optical router model to analyze crosstalk noise, power loss, and SNR in optical routers. Table I lists the notations of the power losses and crosstalk coefficients used in the proposed analytical models in this paper. In this table, L corresponds to different power loss values and X indicates different crosstalk noise coefficients. Since the values of crosstalk coefficients are very small numbers, we ignore orders of crosstalk noise higher than the first-order; $X_i X_j$ or X_i^2 are ignored. We consider the use of a single optical wavelength in this paper.

A. Analytical Models for Photonic Elements

The waveguide crossing is shown in Fig. 1(a). It consists of an input port and three output ports, which are out1, out2, and out3. Given P_{in} as the input power at the input port, we model the crossing loss from the input port to the out1 output port and the generated crosstalk noise at the out2 and out3 output ports in (1a) and (1b), respectively. In these equations, P_{out1}, P_{out2}, and P_{out3}, respectively, indicate the output powers at the out1, out2, and out3 output ports

$$P_{\text{out1}} = L_c P_{\text{in}} \tag{1a}$$
$$P_{\text{out2}} = P_{\text{out3}} = X_c P_{\text{in}}. \tag{1b}$$

The parallel switching element, shown in Fig. 1(c)–(f), is a structure consisting of a miroresonator located between two parallel waveguides. The PSE can be either in the ON or the OFF state. An optical signal with a wavelength different from the resonant frequency of the microresonator (the OFF state) will pass the ring toward the through port, as in Fig. 1(c). By contrast, when the switch is turned on, as in Fig. 1(e), the optical signal will couple into the ring and be directed to the drop port (the ON state). The passing loss and the crosstalk noise at the through and drop ports of the PSE in the OFF state are calculated in (2a) and (2b), respectively. Moreover, when the PSE is in the ON state, (3a) calculates the crosstalk noise at the through port, while (3b) calculates the drop loss of the PSE. In these equations, P_T is the output power at the through port and and P_D is the output power at the drop port

$$P_{T\,\text{pse,off}} = L_{p0} P_{\text{in}} \tag{2a}$$
$$P_{D\,\text{pse,off}} = X_{p0} P_{\text{in}} \tag{2b}$$
$$P_{T\,\text{pse,on}} = X_{p1} P_{\text{in}} \tag{3a}$$
$$P_{D\,\text{pse,on}} = L_{p1} P_{\text{in}}. \tag{3b}$$

Fig. 1(b), (d), and (f) show the interference between two optical signals, from different power sources, while they are passing the same waveguide crossing or parallel switching element. As the figures show, the crosstalk noise from the optical signal $S1$ ($S2$) mixes with the optical signal $S2$ ($S1$) at the $S2_{\text{out}}$ ($S1_{\text{out}}$) output port. Such interferences occur in optical routers when two, or more than two, optical signals simultaneously pass through the same optical router and mix with each other.

The crossing switching element, shown in Fig. 3, consists of a waveguide crossing and a microresonator placed next to the intersection of the crossing. The power loss and crosstalk noise analytical models of the CSE can be derived based on the PSE and the waveguide crossing. Considering the proposed analytical models of the PSE in the OFF state and the waveguide crossing, the output powers at the through port, P_T, the drop port, P_D, and the add port, P_A, of the CSE in the OFF state, as shown in Fig. 3(a), are calculated in (4a)–(4c), respectively. When the CSE is in the ON state, as shown in Fig. 3(b), the output powers can be calculated using the analytical models of the PSE in the ON state and the waveguide crossing as described in (5a) and (5b). As mentioned previously, the crosstalk noise at the add port in the ON state is ignored since we consider the first-order incoherent crosstalk noise. When the CSE is in the OFF state, as indicated in Fig. 3(a), the power loss at the through port, L_{c0}, includes the passing loss caused by the MR and the crossing loss from the waveguide crossing, as described in (4a). Using the same principles, the power loss and crosstalk noise sources in these equations can be explained. Utilizing the proposed models for the basic elements, we model the insertion loss and crosstalk noise in optical routers

$$P_{T\,\text{cse,off}} = L_{c0} P_{\text{in}} = (L_{p0} L_c) P_{\text{in}} \tag{4a}$$
$$P_{D\,\text{cse,off}} = \left(X_{p0} + L_{p0}^2 X_c\right) P_{\text{in}} \tag{4b}$$
$$P_{A\,\text{cse,off}} = X_c L_{p0} P_{\text{in}} \tag{4c}$$
$$P_{T\,\text{cse,on}} = X_{p1} L_c P_{\text{in}} \tag{5a}$$
$$P_{D\,\text{cse,on}} = L_{c1} P_{\text{in}} = (L_{p1}) P_{\text{in}}. \tag{5b}$$

B. Analytical Models for the General 4×4 Optical Router

Optical routers are constructed using BOSEs, waveguide crossings, waveguide bendings, and optical terminators, which are used to keep the light from reflecting back on the transmission line. Fat-tree-based ONoCs use 4×4 optical routers, where each optical router is connected to four neighboring routers through bidirectional channels. We present a general 4×4 optical router model, which can be applied to any

This article has been accepted for inclusion in a future issue of this journal. Content is final as presented, with the exception of pagination.

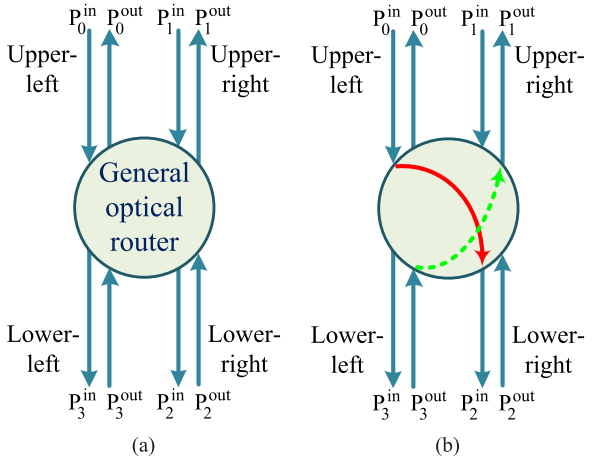

Fig. 4. General 4×4 optical router model proposed for fat-tree-based ONoCs and a status definition in this model. Solid red line: the considered optical signal. Dotted green line: the interfering optical signal. (a) General router model. (b) Router's status example.

other 4×4 optical routers. This way, the proposed analyses at the router and network levels can be adapted to fat-tree-based ONoCs using an arbitrary 4×4 optical router. Fig. 4(a) shows the general optical router model. It has four input and four output ports, which are named as $P^{\text{in\textbackslash out}}_{\text{prt}_{\text{num}}}$ in which the subscript prt_{num} is the port number and is equal to 0 for the upper-left port, 1 for the upper-right port, 2 for the lower-right port, and 3 for the lower-left port. Moreover, the superscript in is used when the port is an input port, while out indicates that the port is an output port. The proposed general router model is based on the optical turnaround routing algorithm. In this routing algorithm, a packet climbs the fat-tree network either upward or downward until it reaches the common ancestor router of the source and the destination of the packet; then, the packet is routed in the opposite direction toward the destination. Turnaround routing is a minimal path adaptive routing algorithm with low-complexity and is free of deadlock and livelock, while not using any global information. The turnaround transmission can occur only between the lower-left and the lower-right ports and vice versa.

The insertion loss of an optical signal traveling from the ith input port toward the jth output port in the optical router $R(x, l)$ is calculated in (6). The insertion loss accounts for the switching loss $S_{Li,j}$, which is the power loss caused by the switching elements (PSEs and CSEs) as well as the waveguide crossings and bendings, and the propagation loss $L_p^{W_{li,j}}$ inside the optical router. In this equation, $W_{li,j}$ is the waveguide's length between the ith input port and the jth output port, while L_p, as listed in Table I, is the propagation loss. k is the number of processor cores

$$L_{i,j}(x,l) = \begin{cases} S_{Li,j}(x,l) L_p^{W_{li,j}(x,l)+2H_l} & \text{destination} \\ S_{Li,j}(x,l) L_p^{W_{li,j}(x,l)+H_l} & \text{otherwise} \end{cases}$$
$$i, j \in \{0, \ldots, 3\},\ x \in \left\{1, \ldots, \frac{k}{2}\right\},\ l \in \{1, \ldots, \log_2 k - 1\}. \quad (6)$$

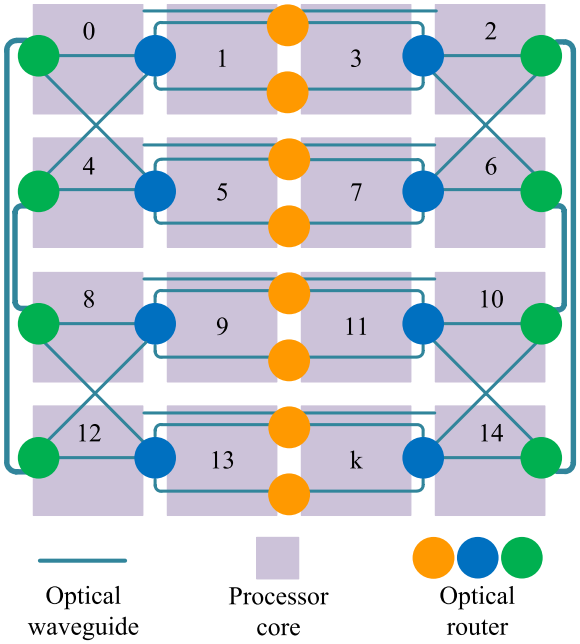

Fig. 5. Optimized fat-tree floorplan proposed in [10].

The propagation loss at the network level is considered in the proposed router model. Considering the waveguide, whose length is H_l, that connects the optical router $R(x, l)$ to a neighboring router or a processor core, we add the propagation loss of either $L_p^{H_l}$, when the current optical router is not the destination, or $L_p^{2H_l}$, when the current router is the destination, to the propagation loss analysis at the router level, as described in (6). In the optimized floorplan of fat-tree-based ONoCs, H_l can be approximated using (7). In this equation, S is the chip size in cm^2, while R and C are the number of processor cores located, respectively, in a row and a column of the optimized floorplan of fat-tree-based ONoCs (see Fig. 5)

$$H_l \cong \sqrt{\frac{S}{R \times C}}. \quad (7)$$

The worst-case crosstalk noise analysis at the destination of an optical link is a result of considering the worst-case configurations of the optical routers on that link at the network level. Therefore, we define the router status for optical routers to determine the router's configuration while optical signals passing the optical router. In this paper, the optical signal which we study the crosstalk noise at its output is called the considered optical signal, while the optical signal which introduces crosstalk noise to the considered optical signal is called the interfering optical signal. With the turnaround routing algorithm, the router status is defined in (8), in which the considered optical signal is travelling from the ith input port toward the jth output port and the other optical signals are interfering with the considered optical signal. In this equation, I^{in}_{ul}, I^{in}_{ur}, I^{in}_{lr}, and I^{in}_{ll} are the input ports associated with the output ports I^{out}_0, I^{out}_1, I^{out}_2, and I^{out}_3, respectively. -1 shows that the output port is free. By way of example, as shown in Fig. 4(b), $s_{0,2}(x,l)(I^{\text{in}}_{-1}, I^{\text{in}}_3, I^{\text{in}}_0, I^{\text{in}}_{-1})$ indicates that the considered optical signal is traveling from the upper-left

This article has been accepted for inclusion in a future issue of this journal. Content is final as presented, with the exception of pagination.

input port toward the lower-right output port, $i = 0$, $j = 2$, and $lr = 0$, while there is another interfering optical signal from another optical power source that is traveling from the lower-left input port toward the upper-right output port, $ur = 3$, and mixes with the considered optical signal, introducing crosstalk noise to it in the optical router *R(x, l)*. Furthermore, it shows that no signal exists at the output ports of the upper-left and lower-left ports, $ul = ll = -1$

$$\begin{aligned} s_{i,j}(x,l) = (I_{ul}^{\text{in}}, I_{ur}^{\text{in}}, I_{lr}^{\text{in}}, I_{ll}^{\text{in}}) & \quad ul \in \{-1,2,3\} \\ & \quad ur \in \{-1,2,3\} \\ & \quad lr \in \{-1,0,1,3\} \\ & \quad ll \in \{-1,0,1,2\} \\ i,j \in \{0,\ldots,3\} & \\ x \in \left\{1,\ldots,\frac{k}{2}\right\} & \\ l \in \{1,\ldots,\log_2 k - 1\}. & \end{aligned} \tag{8}$$

When an optical signal with a power of $P_i^{\text{in}}(x,l)$ enters the *i*th input port of the optical router *R(x, l)*, the output power $P_{i,j}^{\text{out}}(x, l)$ at the j output port of the optical router can be calculated using (9). $L_{i,j}(x,l)$, as defined in (6), is the insertion loss of the optical signal in the optical router $R(x,l)$. For example, using (9) and based on Fig. 4(b), the optical power at the lower-right output port is $P_{0,2}^{\text{out}} = P_0^{\text{in}} L_{0,2}$, in which P_0^{in} is the optical power at the upper-left input port and $L_{0,2}$ is the insertion loss from the upper-left input port toward the lower-right output port

$$\begin{aligned} P_{i,j}^{\text{out}}(x,y) &= P_i^{\text{in}}(x,l) L_{i,j}(x,l) \\ i,j &\in \{0,\ldots,3\} \\ x &\in \left\{1,\ldots,\frac{k}{2}\right\} \\ l &\in \{1,\ldots,\log_2 k - 1\}. \end{aligned} \tag{9}$$

Considering the optical router $R(x,\ l)$ and its current status $s_{i,j}(x,l)$, the crosstalk noise $n_{i,j}(x,l,s_{i,j}(x,l))$ added to the considered optical signal traveling from the *i*th input port to the *j*th output port is calculated in (10). In this equation, $P_m^{\text{in}}(x,l)$ is the optical power of the interfering optical signal, which mixes with the considered optical signal through the *m*th input port, and $X_{i,j,m}(s_{i,j}(x,l))$ is the the coefficient for the crosstalk noise introduced by the interfering optical signal to the considered optical signal in the router *R(x, l)*. For instance, applying this equation to Fig. 4(b), the crosstalk noise added to the considered optical signal can be defined as $n_{0,2} = P_3^{\text{in}} X_{0,2,3}$, where P_3^{in} is the power of the interfering optical signal at the Lower-left input port and $X_{0,2,3}$ is the coefficient for crosstalk noise introduced to the considered optical signal. According to Fig. 4(b), it is obvious that $X_{0,2,0} = X_{0,2,1} = X_{0,2,2} = 0$

$$\begin{aligned} n_{i,j}(x,l,s_{i,j}(x,l)) &= \sum_{m=0}^{3} \left(P_m^{\text{in}}(x,l) X_{i,j,m}(s_{i,j}(x,l)) \right) \\ i,j &\in \{0,\ldots,3\} \\ x &\in \{1,\ldots,\frac{k}{2}\} \\ l &\in \{1,\ldots,\log_2 k - 1\}. \end{aligned} \tag{10}$$

SNR determines the feasibility of ONoCs. It can be defined as the ratio of the signal power to the power of the crosstalk noise corrupting the signal, as described in (11), in which P_S is the optical signal power and P_N is the crosstalk noise power

$$\text{SNR} = 10 \log \left(\frac{P_S}{P_N} \right). \tag{11}$$

IV. Worst-Case SNR Analysis in Fat-Tree-Based ONoCs

The floorplan and the topology of the optimized fat-tree-based ONoCs are shown in Figs. 5 and 7, respectively. The topology comprises an upper and a lower subnetwork. Optical routers at different levels are the same, but are illustrated in different colors to facilitate the matching between the floorplan and the topology. It is worth mentioning that the optical routers in the lower subnetwork are flipped over so that the upper-left and the upper-right ports are now directed downward, while the other two ports, lower-left and lower-right, are directed upward in the lower subnetwork. The optical links in the floorplan are all bidirectional, but are merged as a single link. Some parameters in fat-tree-based ONoCs are predefined for convenience while analyzing the SNR. Regarding Figs. 5 and 7, when the number of processor cores is equal to k, the number of possible levels in fat-tree-based ONoCs, level, is calculated in (12). We assume that the processor cores are located at level zero. The maximum number of waveguide crossings between level *l-1* and level l, $W_{\max}[l-1:l]$, is calculated in (13), while the minimum number of waveguide crossings between any two levels is always equal to zero, as mentioned in (14). Using (13), the maximum number of waveguide crossings between level l_1 and level l_2, $W_{\max}[l_1:l_2]$, can be defined as (15). According to (14) and (15), the average number of waveguide crossings between levels l_1 and l_2, $W_{\text{avg}}[l_1:l_2]$, is calculated in (16). It is assumed that there are two waveguide bendings between every two optical routers in the floorplan of fat-tree-based ONoCs, while each processor core is connected to a first-level optical router with a single waveguide bending. Hence, the number of waveguide bendings from a processor core to the optical router located at level l, $B_n[0,l]$, can be calculated as (17). In all the equations, we have $l_2 > l_1$ as well as $l_1 > 0$ and $l > 0$

$$\text{level} = \log_2 k - 1 \tag{12}$$

$$W_{\max}[l-1:l] = 2^{l-1} - 2 \tag{13}$$

$$W_{\min}[l_1:l_2] = 0 \tag{14}$$

$$W_{\max}[l_1:l_2] = \sum_{i=l_1+1}^{l_2} \left(2^{i-1} - 2\right) \tag{15}$$

$$W_{\text{avg}}[l_1:l_2] = \frac{1}{2}\left(\sum_{i=l_1+1}^{l_2} \left(2^{i-1} - 2\right) \right) \tag{16}$$

$$B_n[0:l] = 2l - 1. \tag{17}$$

By means of the proposed analytical models for the basic photonic devices and the general optical router model, we

This article has been accepted for inclusion in a future issue of this journal. Content is final as presented, with the exception of pagination.

analyze the worst-case SNR in fat-tree-based ONoCs. To find and analyze the worst-case SNR link in fat-tree-based ONoCs, some steps are carried out: 1) we present the worst-case crosstalk noise patterns employed to find and analyze the worst-case SNR link in fat-tree-based ONoCs; 2) using the proposed worst-case crosstalk noise patterns, the optical links having the worst-case SNR compared with the other links of the same length or hop-length are found; and 3) the worst-case SNR of different longest optical links are analyzed and compared to find the worst-case SNR link candidates. It is worth mentioning that throughout steps one to three, we consider all the possible communication paths as well as traffic allocations and dynamic workloads in the network to find and analyze the worst-case SNR link. The analyses at the device and optical router levels can be applied to other ONoC architectures as long as a 4×4 optical router is used.

A. Worst-Case Crosstalk Noise Patterns in Fat-Tree-Based ONoCs

We start the worst-case crosstalk noise analyses in fat-tree-based ONoCs by presenting some assumptions. Firstly, the insertion loss from the ith input port to the jth output port is unique among different optical routers in different locations. Hence, $L_{i,j}(x,l)$ is simplified as $L_{i,j}$, which is the insertion loss from the ith input port toward the jth output port regardless of the optical router location, as shown in (18). The second assumption is that the injecting laser power at different processor cores, while generating the optical signal, is the same and consistent. Finally, (19) explains the last assumption. In this equation, in is the input port which is connected to a processor core at level one. As mentioned previously, the proposed analyses consider the first-order crosstalk noise, as shown in (20)

$$\begin{aligned} L_{i,j}(x_0,l_0) &= L_{i,j}(x_1,l_1) = L_{i,j} \\ x_0, x_1 &\in \left\{1,\ldots,\frac{k}{4}\right\}, l_0, l_1 \in \{1,\ldots,\log_2 k-1\} \\ i, j &\in \{0,\ldots,3\} \qquad (18) \\ L_{\text{in},j_0} &\geq L_{\text{in},j_1} L_{(j_1+1)\bmod 3+1,j_0} \\ j_0, j_1 &\in \{0,\ldots,3\} \qquad (19) \\ X_{i_0,j_0,m_0} X_{i_1,j_1,m_1} &\approx 0 \\ i_0, j_0, m_0, i_1, j_1, m_1 &\in \{0,\ldots,3\}. \qquad (20) \end{aligned}$$

The worst-case crosstalk noise patterns are presented to help find and analyze the worst-case SNR among optical links with the same hop length, but different paths, in fat-tree-based ONoCs. Fig. 6 shows 10 different worst-case crosstalk noise patterns, while each pattern shows the general optical router $R(x,l)$ under its worst-case status $ws_{i,j}(x,l)$. The worst-case crosstalk noise patterns can be used to realize different traffic allocations and dynamic loads in the network. Utilizing (10) for each pattern, we define $n_{i,j,m}(x,l,ws_{i,j}(x,l))$ as the worst-case crosstalk noise caused by the interfering optical signal through the mth input port, which is added to the considered optical signal travelling from the ith input port toward the jth output port in the optical router $R(x,l)$ under the worst-case status $ws_{i,j}(x,l)$. Without loss of generality, due to the symmetric structure of optical routers, to simplify the resultant equations we assume that the insertion loss between different input and output pairs is the same, $L_{i,j} = L$. When the interfering optical signals mix with the considered optical signal through one of the upper input ports, $m = 0$ or $m = 1$, (21), shown at the bottom of the page, calculates the resulting crosstalk noise power received at the output port of the optical router. Furthermore, (22), shown at the bottom of the page, defines the crosstalk noise power caused by the interfering optical signals through one of the lower input ports, $m = 2$ or $m = 3$. In these equations, $X_{i,j,m}$ is the crosstalk noise coefficient, while the terms before that correspond to the signal power of the interfering optical signal [P_m^{in} in (10)]. P_{in} is the injection power at the source processor core. For example, in Fig. 6(a), the considered optical signal, travelling from the upper-left input port, $i = 0$, toward the lower-right output port, $j = 2$, is interfered with the other optical signals through the upper-right, lower-right, and lower-left input ports. The power of the crosstalk noise at the output port of the considered optical signal in Fig. 6(a) is shown in (23)

$$\begin{aligned} &n_{0,2,m}(x,l,ws_{0,2}(x,l)) \\ &\quad = P_{\text{in}} L^{l+1} L_b^{B_n[0:l+2]} L_c^{W_{\text{avg}}[2:l+1]+W_{\text{avg}}[l:l+1]} X_{0,2,1} \\ &\qquad + \left(P_{\text{in}} L^{l-1} L_b^{B_n[0:l]} L_c^{W_{\text{avg}}[2:l]}\right)(X_{0,2,2} + X_{0,2,3}). \qquad (23) \end{aligned}$$

B. Determining the Worst-Case SNR Link Among Links of the Same Length

To find the worst-case SNR link candidates, two major conditions need to be simultaneously considered. The worst-case SNR link should suffer from high power loss, and, at the same time, the accumulated crosstalk noise on this link and received at its destination should be the worst-case. The crosstalk noise is introduced by both the optical signal on the worst-case SNR link and the optical signals, whose wavelengths are the same as the considered optical signal, on the other links crossing the worst-case SNR link through optical routers. Considering the aforementioned conditions, different longest optical links are appropriate candidates to be the worst-case SNR link because while they are passing through a large number of optical routers, not only do they suffer from high power loss, but they also simultaneously experience high crosstalk noise. However, the number of different longest optical links is not a consistent small number; in fat-tree-based

$$n_{i,j,0|1}(x,l,ws_{i,j}(x,l)) = \begin{cases} P_{\text{in}} L^{l+1} L_b^{B_n[0:l+2]} L_c^{W_{\text{avg}}[2:l+1]+W_{\text{avg}}[l:l+1]} X_{i,j,0|1} & l \neq \log_2 k - 1 \\ P_{\text{in}} L^{l} L_b^{B_n[0:l+1]} L_c^{W_{\text{avg}}[2:l]} X_{i,j,0|1} & l = \log_2 k - 1 \end{cases} \qquad (21)$$

$$n_{i,j,2|3}(x,l,ws_{i,j}(x,l)) = P_{\text{in}} L^{l-1} L_b^{B_n[0:l]} L_c^{W_{\text{avg}}[2:l]} X_{i,j,2|3} \qquad (22)$$

This article has been accepted for inclusion in a future issue of this journal. Content is final as presented, with the exception of pagination.

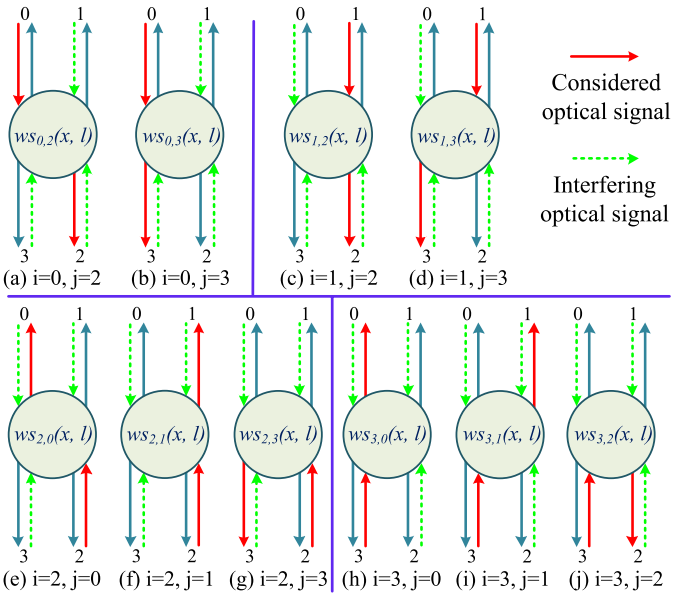

Fig. 6. Worst-case crosstalk noise patterns proposed to analyze the worst-case SNR in fat-tree-based ONoCs.

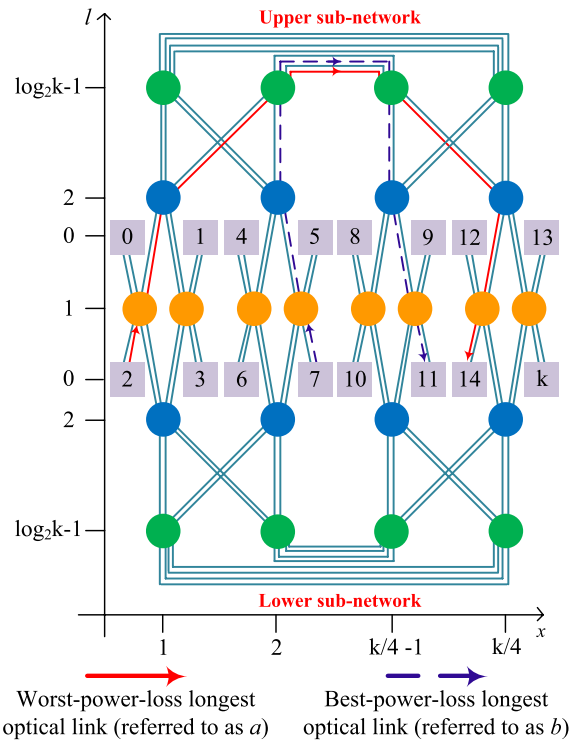

Fig. 7. Worst-case power loss and the best-case power loss longest optical links in fat-tree-based ONoCs.

ONoCs $k2^{(\log_2 k-2)}$ longest optical links exist in the network. In this subsection, we analytically find the worst-case SNR link among optical links of equal hop-length, but different paths. The longest optical link is considered as an example in this subsection.

Fig. 7 shows two longest optical links, in which the solid line shows the worst-case power loss optical link, referred to as optical link a, while the dashed line is the optical link suffering from the least power loss, referred to as optical link b, in the network. Applying the proposed crosstalk noise patterns to these longest optical links, both optical links experience the same amount of crosstalk noise accumulated at different optical routers along their paths. However, since the optical link a suffers from higher power loss compared with the optical link b, the crosstalk noise power received at the destination of the former optical link is lower. In other words, the crosstalk noise power received at the destination of the link a is the lowest among all the longest optical links, while the crosstalk noise received at the destination of the optical link b is the highest. Therefore, the SNR of the longest optical links is bounded by the SNR of the optical links a and b, as we will prove shortly. It is worth mentioning that there are six other longest optical links with the same characteristics as those shown in the figure, which will lead us to the same analyses and conclusions proposed in this section.

The power loss of the optical link a, $L^a_{2,k-2}$, is calculated in (24), while (25) shows the power loss of the optical link b, $L^b_{(k/2-1),(k/2+3)}$. In these equations, $L^{a|b}_{c_0,c_1}$ is the power loss from the processor core c_0 to the processor core c_1. Considering (14), it can be seen that $W_{\min}[2:\log_2 k-1]=0$. Based on the SNR definition in (11), the SNR of the optical link a is defined in (26), while (27) is used to calculate the SNR of the optical link b

$$L^a_{2,k-2} = L^{2\log_2 k-2} L_b^{2B_n[0:\log_2 k-1]+2} L_c^{2W_{\max}[2:\log_2 k-1]} \tag{24}$$

$$L^b_{\frac{k}{2}-1,\frac{k}{2}+3} = L^{2\log_2 k-2} L_b^{2B_n[0:\log_2 k-1]+2} L_c^{2W_{\min}[2:\log_2 k-1]} \tag{25}$$

$$\mathrm{SNR}^a_{2,k-2} = 10\log\left(\frac{P_{\text{in}} L^a_{2,k-2}}{F^a(L,L_b,L_c).N^a_{i,j}}\right)$$

where

$$N^a_{i,j} = \left[N^a_{3,1}, N^a_{0,2}, \left(N^a_{0,3}=N^a_{1,3}\right)\right] \tag{26}$$

$$\mathrm{SNR}^b_{\frac{k}{2}-1,\frac{k}{2}+3} = 10\log\left(\frac{P_{\text{in}} L^b_{\frac{k}{2}-1,\frac{k}{2}+3}}{F^b(L,L_b,L_c).N^b_{i,j}}\right)$$

where

$$N^b_{i,j} = \left[\left(N^b_{2,0}=N^b_{2,1}\right), N^b_{1,3}, N^b_{0,2}\right]. \tag{27}$$

In these equations, $F^{a|b}(L,L_b,L_c)$ is the power loss function associated with the crosstalk noise received at the destination of the optical link a or the optical link b. Furthermore, $N^{a|b}_{i,j}$ is the crosstalk noise from different optical routers on the optical link a or b. $F^{a|b}(L,L_b,L_c)$ and $N^{a|b}_{i,j}$ are calculated in Appendix. P_{in} is the injection power at the source processor core. The received crosstalk noise power at the destination of the optical link a or b can be obtained using $F^{a|b}(L,L_b,L_c).N^{a|b}_{i,j}$. Since crosstalk coefficients are very small numbers, we assume that different coefficients are similar and are equal to the arithmetic mean of all the crosstalk noise coefficients, as $X_{i,j,m}=\bar{X}$.

This article has been accepted for inclusion in a future issue of this journal. Content is final as presented, with the exception of pagination.

Regarding the optical link a and (39) in the Appendix, $N^a_{i,j}$ should be defined as $N^a_{i,j} = [N^a_{3,1}, N^a_{0,2}, N^a_{0,3}, N^a_{1,3}]$. However, since $N^a_{0,3} = N^a_{1,3}$, $N^a_{i,j}$ is simplified as shown in (26). Similarly, $N^b_{i,j}$ is simplified as indicated in (27).

The SNR equations of the optical links a and b are compared in (28). With (21) and (22), it can be concluded that $N^a_{i,j} = N^b_{i,j}$. Furthermore, $L^a_{2,k-2}/L^b_{(k/2-1),(k/2+3)}$ can be simplified as $L_c^{2W_{\max}[2:\log_2 k-1]}$ using the power loss definitions in (24) and (25). Eventually, according to (41) and (42) (see Appendix), it can be seen that $L_c^{2W_{\max}[2:\log_2 k-1]} F^b(L, L_b, L_c) < F^a(L, L_b, L_c)$, which leads to the conclusion drawn in (28)

$$\frac{\mathrm{SNR}^a_{2,k-2}}{\mathrm{SNR}^b_{\frac{k}{2}-1,\frac{k}{2}+3}} = \frac{L^a_{2,k-2} F^b(L, L_b, L_c)}{L^b_{\frac{k}{2}-1,\frac{k}{2}+3} F^a(L, L_b, L_c)} \Leftrightarrow \frac{L_c^{2W_{\max}[2:\log_2 k-1]} F^b(L, L_b, L_c)}{F^a(L, L_b, L_c)} < 1. \quad (28)$$

The conclusion made in (28) can be applied to any other longest optical link, let's say the optical link ran, whose power loss is neither the worst nor the best. This conclusion is valid since for the optical link ran, $N^a_{i,j} = N^b_{i,j} = N^{\mathrm{ran}}_{i,j}$. Moreover, for the power loss of the optical link ran, we always have $L^a_{2,k-2} \le L^{\mathrm{ran}}_{c_0,c_1} \le L^b_{(k/2-1),(k/2+3)}$. Therefore, given the number of waveguide crossings met by the optical link ran as L^{ran}_c, one can easily come to the conclusion that $L^{\mathrm{ran}}_c F^b(L, L_b, L_c) \le F^{\mathrm{ran}}(L, L_b, L_c)$, which leads to $\mathrm{SNR}^{\mathrm{ran}} \le \mathrm{SNR}^b_{(k/2-1),(k/2+3)}$, and $L_c^{2W_{\max}[2:\log_2 k-1]} F^{\mathrm{ran}}(L, L_b, L_c) \le L^{\mathrm{ran}}_c F^a(L, L_b, L_c)$, which leads to $\mathrm{SNR}^a_{2,k-2} \le \mathrm{SNR}^{\mathrm{ran}}$, resulting in (29)

$$\mathrm{SNR}^a_{2,k-2} \le \mathrm{SNR}^{\mathrm{ran}}_{c_0,c_1} \le \mathrm{SNR}^b_{\frac{k}{2}-1,\frac{k}{2}+3}. \quad (29)$$

We have proven that among the optical links of the same hop-length, but different paths, the one which suffers from the highest power loss has the worst-case SNR, while the optical link with the least power loss has the best-case SNR in fat-tree-based ONoCs. This finding is used to analyze the worst-case SNR of different longest optical links in the next subsection.

C. Worst-Case SNR Analysis of Different Longest Links

The total number of second longest optical links in fat-tree-based ONoCs is equal to $k2^{\log_2 k-3}$. Applying the conclusion drawn in the previous subsection, those second longest links with the highest power loss have the worst SNR. There are sixteen links among the second longest links which have the maximum power loss, and hence the worst SNR, compared with the others, and four of them are depicted as an example in Fig. 8. Analyzing the SNR of the second longest link, we select the optical link between the processor cores $c_0 = 2$ and $c_1 = k/4+2$ as an example. The analyses for the other fifteen optical links follow the same principle.

The power loss imposed on the second longest optical link is defined in (30). Utilizing the proposed worst-case crosstalk noise patterns in Fig. 6, we analyze the worst-case crosstalk noise accumulated on the second longest optical link in the

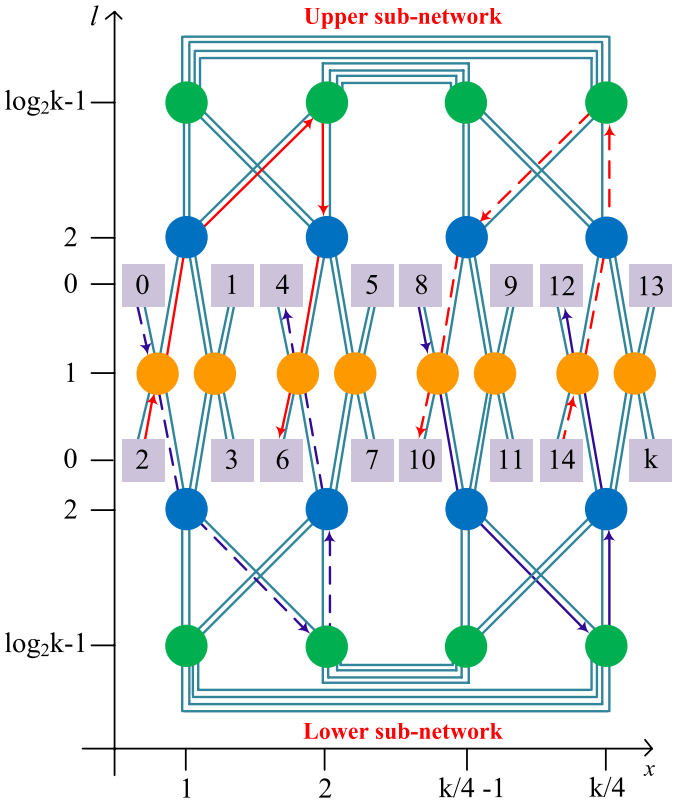

Fig. 8. Four of the worst-case SNR second longest optical links in fat-tree-based ONoCs.

Appendix

$$L^{'}_{2,\frac{k}{4}+2} = L^{2\log_2 k-3} L_b^{2B_n[0:\log_2 k-1]} L_c^{W_{\max}[2:\log_2 k-1]+W_{\max}[2:\log_2 k-2]} \quad (30)$$

$$\mathrm{SNR}^{'}_{2,\frac{k}{4}+2} = 10\log\left(\frac{P_{\mathrm{in}} L^{'}_{2,\frac{k}{4}+2}}{F^{'}(L, L_b, L_c).N^{'}_{i,j}}\right)$$

where

$$N^{'}_{i,j} = [N^{'}_{3,1}, N^{'}_{3,2}, N^{'}_{1,3}] \quad (31)$$

Using (11), (30), and (43) in the Appendix, the worst-case SNR at the destination of the second longest optical link is calculated in (31). In this equation, $F^{'}(L, L_b, L_c).N^{'}_{i,j}$, in which $F^{'}(L, L_b, L_c)$ is the power loss function associated with the accumulated crosstalk noise on the second longest optical link, $N^{'}_{i,j}$, is the received crosstalk noise power at the destination of the link. $F^{'}(L, L_b, L_c)$ and $N^{'}_{i,j}$ are defined in the Appendix.

Comparing the SNR of the first longest link with that of the second longest link, we define the auxiliary parameters α_1 to α_4 as shown in

$$\alpha_1 = L^{\log_2 k-1} L_b^{Bn[0:\log_2 k-1]+2} L_c^{W_{\max}[2:\log_2 k-1]} \quad (32a)$$

$$\alpha_2 = f^a_1 - \alpha_1 \quad (32b)$$

$$\alpha_3 = L^{\log_2 k-2} L_b^{Bn[0:\log_2 k-1]} L_c^{W_{\max}[2:\log_2 k-1]} \quad (32c)$$

$$\alpha_4 = (f^a_2 + f^a_3) - \alpha_3. \quad (32d)$$

This article has been accepted for inclusion in a future issue of this journal. Content is final as presented, with the exception of pagination.

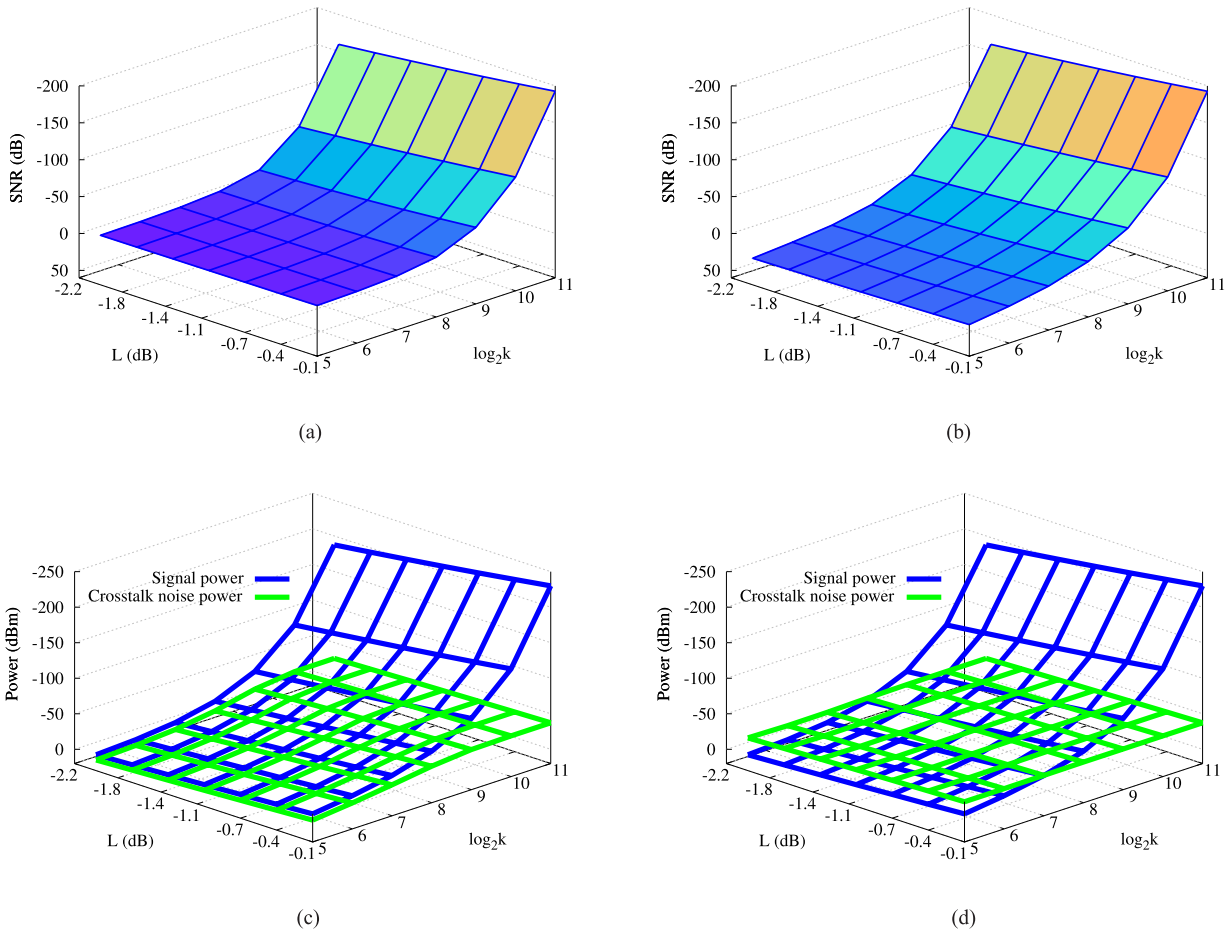

Fig. 9. Worst-case SNR, signal power, and crosstalk noise power in fat-tree-based ONoCs using an arbitrary 4×4 optical router. (a) $\bar{X} = -5$ dB. (b) $\bar{X} = -30$ dB. (c) $\bar{X} = -5$ dB. (d) $\bar{X} = -30$ dB.

Simplifying the SNR equations of the first and the second longest links, we apply the above parameters to their SNR equations as shown in (33) and (34) at the bottom of the page, respectively. In the former equation, the SNR of the first longest optical link is further simplified with $N^a_{0,2} = N^a_{0,3}$. According to (21) and (22), it can be seen that $N^a_{3,1} = N^{'}_{3,1}$, $N^a_{0,2} > N^{'}_{3,2}$ and $N^a_{0,2} = N^{'}_{1,3}$. Furthermore, the relationship between the power loss of the first longest link, shown in (24), and the second longest link, defined in (30), can be considered as (35)

$$\frac{L^a_{2,k-2}}{L^{'}_{2,\frac{k}{4}+2}} = LL_b^2 L_c^{2^{\log_2 k-2}-2}. \tag{35}$$

Utilizing the above relations and simplifications, we prove that the SNR of the first longest optical link is smaller than that of the second longest link, as described in (36)

$$\begin{aligned} \mathrm{SNR}^a_{2,k-2} &< \mathrm{SNR}^{'}_{2,\frac{k}{4}+2} \Leftrightarrow \alpha_2 N^{'}_{3,1} + \alpha_3 LL_b^2 N^{'}_{3,2} \\ &\quad + \alpha_4 LL_b^2 L_c^{2^{\log_2 k-2}-2} N^{'}_{1,3} \\ &< \alpha_1 N^a_{3,1} + \alpha_2 N^a_{3,1} + \alpha_3 N^a_{0,2} + \alpha_4 N^a_{0,2}. \end{aligned} \tag{36}$$

Comparing the SNR of the optical links shorter than the second longest link results in the conclusion that the SNR of those links reduces as the link's hop-length decreases. In other words, the SNR of those optical links depends only on the power loss of the link; the shorter the optical link, the better the SNR is. Therefore, according to the conclusion drawn in (36), we have demonstrated that the worst-case SNR link in fat-tree-based ONoCs using an arbitrary 4×4 optical router is one of the four longest optical links, among the total number of $k2^{(\log_2 k-2)}$ possible longest optical links, which suffer from

$$\mathrm{SNR}^a_{2,k-2} = 10 \log \left(\frac{P_{\mathrm{in}} L^a_{2,k-2}}{\alpha_1 N^a_{3,1} + \alpha_2 N^a_{3,1} + \alpha_3 N^a_{0,2} + \alpha_4 N^a_{0,2}} \right) \tag{33}$$

$$\mathrm{SNR}^{'}_{2,\frac{k}{4}+2} = 10 \log \left(\frac{P_{\mathrm{in}} L^{'}_{2,\frac{k}{4}+2}}{\alpha_2 L^{-1} L_b^{-2} L_c^{2-2^{\log_2 k-2}} N^{'}_{3,1} + \alpha_3 L_c^{2-2^{\log_2 k-2}} N^{'}_{3,2} + \alpha_4 N^{'}_{1,3}} \right) \tag{34}$$

This article has been accepted for inclusion in a future issue of this journal. Content is final as presented, with the exception of pagination.

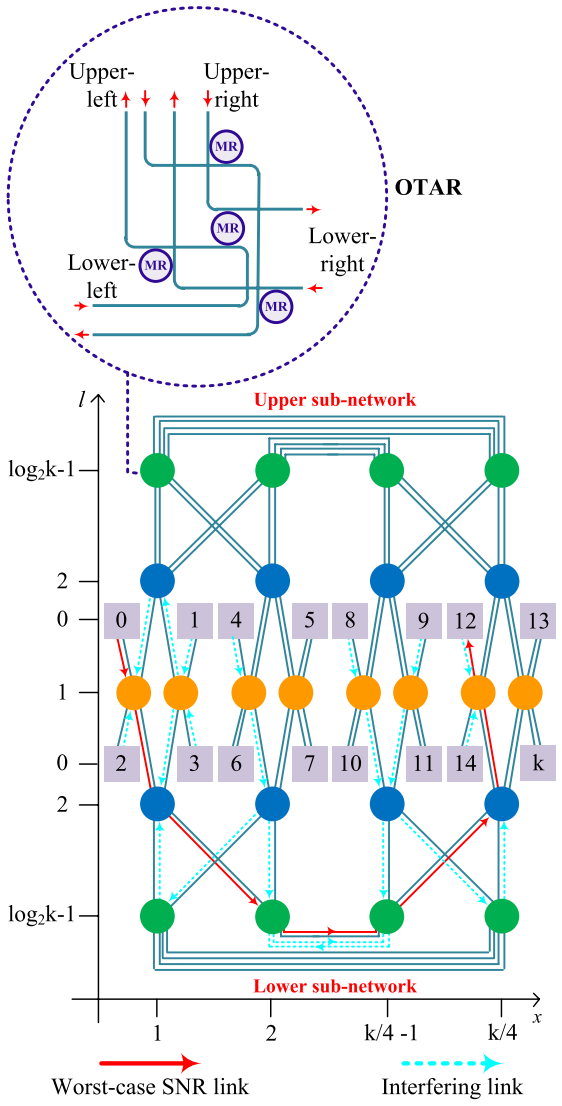

Fig. 10. Worst-case SNR link in fat-tree-based ONoCs using the OTAR.

the highest power loss in the network. Since the proposed analyses are not aimed at a specific SNR, they are applicable to fat-tree-based ONoCs using different photodetectors with a variety of sensitivities.

The worst-case SNR in fat-tree-based ONoCs was quantitatively simulated in MATLAB based on (26) under two different arithmetic mean values of the crosstalk coefficient, $\bar{X}$, as shown in Fig. 9(a), where $\bar{X} = -5$ dB, and Fig. 9(b), where $\bar{X} = -30$ dB. The z-axis is reversed to better show the results. According to these figures, the SNR slightly decreases as the loss value L increases, while it exponentially diminishes with an increase in the number of processor cores, k. When the number of processor cores increases, the worst-case SNR link passes through more optical routers, resulting in higher power loss and accumulating more crosstalk noise power, and hence worse SNR. However, given a fixed value of k, the increase in L attenuates both the signal power and crosstalk noise power, resulting in a slight variation in the SNR. Even when $5 \leq k \leq 8$, the high power loss and crosstalk noise power result in a low SNR. Another important observation is the substantial reduction of the SNR when $\bar{X}$ increases. In Fig. 9(a), for example, the SNR is markedly lower compared with Fig. 9(b), in which $\bar{X}$ is -30 dB. The reason is that when $\bar{X}$ is higher, more crosstalk noise will be accumulated on the worst-case link, which ultimately increases the crosstalk noise power received at the destination of the worst-case SNR link. The quantitative simulations of the worst-case signal power and crosstalk noise power in fat-tree-based ONoCs are illustrated in Fig. 9(c), where $\bar{X} = -5$ dB, and Fig. 9(d), where $\bar{X} = -30$ dB. According to these figures and (24), the signal power reduces exponentially when the number of processor cores increases, while it decreases slightly when the loss value L rises. However, there is a small reduction in the crosstalk noise power when k and L increase. Moreover, comparing the two figures, while the signal power remains the same, a considerable increase in the crosstalk noise power is obvious when $\bar{X}$ increases.

V. Case Study

Leveraging the proposed analytical models, we study the worst-case SNR in fat-tree-based ONoCs using an optical turnaround router. The OTAR is shown in Fig. 10. It is a deadlock and livelock free four by four optical router, which adaptively routes the packets based on the optical turnaround routing algorithm. We analyzed and compared the SNR of the worst-case SNR link candidates in the network, and we found that the optical link from the processor core $c_0 = 0$ to the processor core $c_1 = k - 4$ has the worst-case SNR. Fig. 10 shows the worst-case SNR optical link in fat-tree-based ONoCs using the OTAR. In this figure, the solid line is the worst-case SNR link, while the dotted lines indicate the interfering optical links which introduce crosstalk noise to the worst-case SNR optical link. Considering all of the possible traffic allocations and dynamic loads, the noise introduction links are determined in such a way as to guarantee the worst-case crosstalk noise power received at the destination of the considered optical signal.

The worst-case signal power in fat-tree-based ONoCs using the OTAR is calculated in (37), shown at the bottom of the page. In this equation, the seven terms on the right-hand side represent the injection power at the source processor core, P_{in}, and insertion losses at the optical routers located on the worst-case optical link. The worst-case SNR in fat-tree-based ONoCs using the OTAR is analyzed in (38), shown at the bottom of the page, in which the power loss

$$PL_{w\text{case}} = P_{\text{in}} L_{0,2} L_{2,0}^{\log_2 k-1} L_{1,3}^{\log_2 k-3} L_{1,2} L_b^{2Bn[0:\log_2 k-1]+2} L_c^{2W_{\max}[2:\log_2 k-1]} \tag{37}$$

$$\text{SNR}_{w\text{case}} = 10 \log \left(\frac{PL_{w\text{case}}}{F^D_{w\text{case}}(L, L_b, L_c) N^D_{i,j\ w\text{case}} + F^U_{w\text{case}}(L, L_b, L_c) N^U_{i,j\ w\text{case}}} \right) \tag{38}$$

This article has been accepted for inclusion in a future issue of this journal. Content is final as presented, with the exception of pagination.

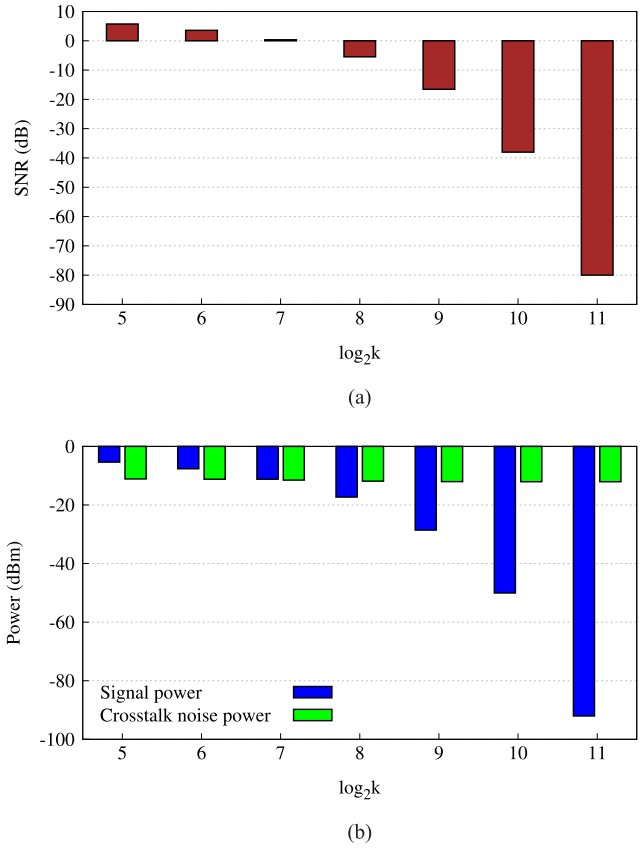

Fig. 11. Worst-case (a) SNR and (b) signal power, and crosstalk noise power in fat-tree-based ONoCs using the OTAR.

functions $F^{D}_{w\text{case}}(L, L_b, L_c)$ and $F^{U}_{w\text{case}}(L, L_b, L_c)$ can be easily calculated based on (37). $N^{D}_{i,j\,w\text{case}}$ and $N^{U}_{i,j\,w\text{case}}$, which are the worst-case crosstalk noise added to the worst-case SNR link, are calculated in the Appendix.

We integrated the proposed worst-case analyses into the novel crosstalk and loss analysis platform, called CLAP [19], [25], and calculated the worst-case SNR, signal power, and crosstalk noise power in fat-tree-based ONoCs using the OTAR. Referring to the notations in Table I, we employed a waveguide crossing with $L_c = -0.04$ dB and $X_c = -40$ dB [14]. Moreover, L_{p0}, L_{p1}, X_{p0}, and X_{p1} are -0.005 dB, -0.5 dB, -20 dB, and -25 dB, respectively [20]. L_b is equal to -0.005 dB/90° and L_p is -0.274 dB/cm [26], [27]. Fig. 11(a) indicates the worst-case SNR in fat-tree-based ONoCs using the OTAR. As the figure indicates, the worst-case SNR reduces exponentially as the number of processor cores increases. An important observation is that when the number of processor cores is larger than $k = 2^7$, the SNR is smaller than zero, which is a result of high crosstalk noise power and power loss. The worst-case signal power and crosstalk noise power in fat-tree-based ONoCs using the OTAR are shown in Fig. 11(b). The signal power decreases exponentially as the number of processor cores increases; meanwhile, the crosstalk noise power remains almost constant under different values of k, while there is a slight reduction in the crosstalk noise power as the network scales. The minor reduction in the crosstalk noise power is because of the higher power loss at the destination of the worst-case SNR link when the network size scales. In other words, when the number of processor cores increases, the power loss of the link rises as well, which attenuates both the signal power and the crosstalk noise power received at the destination. As also seen in Fig. 11(b), when the number of processor cores is larger than $k = 2^7$, the crosstalk noise power exceeds the signal power. For example, when k equals 2^6, the worst-case SNR, signal power, and crosstalk noise power are equal to 3.6 dB, -7.6 dBm, and -11.2 dBm, respectively. However, when the number of processor cores increases to 2^8, these parameters change to -5.5 dB, -17.3 dBm, and -11.9 dBm. The case study results show perfect consistency with those from the general optical router model, which indicates the validity of our general model analyses.

VI. Conclusion

Basic photonic devices, which are the basic components widely used in construction of ONoCs, experience inevitable power loss and crosstalk noise. As a result, the accumulative crosstalk noise diminishes the SNR and restricts the network scalability in ONoCs. For the first time, this paper analyzes and models the worst-case crosstalk noise and SNR in fat-tree-based ONoCs. We hierarchically conduct the formal analyses at the basic photonic devices level, then at the optical router level, and finally at the network level. The proposed analyses are based on a 4×4 general optical router model, which help the proposed analyses be adapted to fat-tree-based ONoCs using an arbitrary 4×4 optical router. We propose the worst-case crosstalk noise patterns in fat-tree-based ONoCs and apply them to find the worst-case SNR link among different longest optical links. The analyses prove that the worst-case SNR link in fat-tree-based ONoCs is among the four possible longest optical links that suffer from the highest power loss in the network. The quantitative simulation results show the critical behavior of crosstalk noise in fat-tree-based ONoCs; the SNR reduces exponentially owing to the high crosstalk noise power and power loss. Leveraging the proposed analytical models, the worst-case SNR, signal power, and crosstalk noise power are analyzed in fat-tree-based ONoCs using an OTAR as a case study. We find that the number of processor cores in fat-tree-based ONoCs is restricted to 128 because of the high crosstalk noise power; the crosstalk noise power exceeds the signal power when the number of processor cores is larger than 128.

Appendix

Utilizing the proposed worst-case crosstalk noise patterns in Fig. 6, we analyze the worst-case crosstalk noise added at different optical routers located on the optical link a, $N^{a}_{i,j}(x, l, ws_{i,j}(x, l))$, and b, $N^{b}_{i,j}(x, l, ws_{i,j}(x, l))$ (shown in Fig. 7) in (39) and (40), shown at the top of the next page, respectively. Moreover, the power loss functions associated with the crosstalk noise received at the destination of the optical signal a, $F^{a}(L, L_b, L_c)$, and the optical signal b, $F^{b}(L, L_b, L_c)$, are defined in (41) and (42), shown at the top of the next page, respectively. The worst-case crosstalk noise mixing with the second longest optical link through the optical routers on the link, $N^{'}_{i,j}(x, l, ws_{i,j}(x, l))$, is analyzed

This article has been accepted for inclusion in a future issue of this journal. Content is final as presented, with the exception of pagination.

$$N^a_{i,j}(x,l,ws_{i,j}(x,l))$$
$$= \begin{cases} n_{3,1,0}(x,l,ws_{3,1}(x,l)) + n_{3,1,1}(x,l,ws_{3,1}(x,l)) + n_{3,1,2}(x,l,ws_{3,1}(x,l)) & i=3, j=1, 1 \le x \le \frac{k}{8}, 1 \le l \le \log_2 k - 1 \\ n_{0,2,1}(x,l,ws_{0,2}(x,l)) + n_{0,2,2}(x,l,ws_{0,2}(x,l)) + n_{0,2,3}(x,l,ws_{0,2}(x,l)) & i=0, j=2, \frac{k}{8} < x < \frac{k}{4}, 2 < l \le \log_2 k - 1 \\ n_{0,3,1}(x,l,ws_{0,3}(x,l)) + n_{0,3,2}(x,l,ws_{0,3}(x,l)) + n_{0,3,3}(x,l,ws_{0,3}(x,l)) & i=0, j=3, x=\frac{k}{4}, l=2 \\ n_{1,3,0}(x,l,ws_{1,3}(x,l)) + n_{1,3,2}(x,l,ws_{1,3}(x,l)) + n_{1,3,3}(x,l,ws_{1,3}(x,l)) & i=1, j=3, x=\frac{k}{2}-1, l=1 \end{cases} \quad (39)$$

$$N^b_{i,j}(x,l,ws_{i,j}(x,l))$$
$$= \begin{cases} n_{2,0,0}(x,l,ws_{2,0}(x,l)) + n_{2,0,1}(x,l,ws_{2,0}(x,l)) + n_{2,0,3}(x,l,ws_{2,0}(x,l)) & i=2, j=0, x=\frac{k}{4}, l=1, x=\frac{k}{8}, l=\log_2 k - 1 \\ n_{2,1,0}(x,l,ws_{2,1}(x,l)) + n_{2,1,1}(x,l,ws_{2,1}(x,l)) + n_{2,1,3}(x,l,ws_{2,1}(x,l)) & i=2, j=1, x=\frac{k}{8}, 2 \le l < \log_2 k - 1 \\ n_{1,3,1}(x,l,ws_{1,3}(x,l)) + n_{1,3,2}(x,l,ws_{1,3}(x,l)) + n_{1,3,3}(x,l,ws_{1,3}(x,l)) & i=1, j=3, x=\frac{k}{8}+1, 2 < l \le \log_2 k - 1 \\ n_{0,2,1}(x,l,ws_{0,2}(x,l)) + n_{0,2,2}(x,l,ws_{0,2}(x,l)) + n_{0,2,3}(x,l,ws_{0,2}(x,l)) & i=0, j=2, x=\frac{k}{8}+1, l=2, x=\frac{k}{4}+2, l=1 \end{cases} \quad (40)$$

$$F^a(L,L_b,L_c) = [f^a_1, f^a_2, f^a_3]$$
$$= \left[\sum_{i=1}^{\log_2 k-1} \left(L^{2\log_2 k-2-i} L_b^{2B_n[0:log_2 k-1]-B_n[0:i]+2} L_c^{W_{\max}[2:log_2 k-1]+W_{\max}[i-1:\log_2 k-1]} \right), \sum_{i=3}^{\log_2 k-1} (L^{i-1} L_b^{Bn[0:i]} L_c^{W_{\max}[2:i]}), LL_b^3 + L_b \right] \quad (41)$$

$$F^b(L,L_b,L_c) = [f^b_1, f^b_2, f^b_3] = \left[\sum_{i=1}^{\log_2 k-1} (L^{2\log_2 k-2-i} L_b^{2B_n[0:\log_2 k-1]-B_n[0:i]+2}), \sum_{i=3}^{\log_2 k-1} (L^{i-1} L_b^{Bn[0:i]}), LL_b^3 + L_b \right] \quad (42)$$

$$N'_{i,j}(x,l,ws_{i,j}(x,l))$$
$$= \begin{cases} n_{3,1,0}(x,l,ws_{3,1}(x,l)) + n_{3,1,1}(x,l,ws_{3,1}(x,l)) + n_{3,1,2}(x,l,ws_{3,1}(x,l)) & i=3, j=1, 1 \le x < \frac{k}{8}, 1 \le l < \log_2 k - 1 \\ n_{3,2,0}(x,l,ws_{3,2}(x,l)) + n_{3,2,1}(x,l,ws_{3,2}(x,l)) + n_{3,2,2}(x,l,ws_{3,2}(x,l)) & i=3, j=2, x=\frac{k}{8}, l=\log_2 k - 1 \\ n_{1,3,0}(x,l,ws_{1,3}(x,l)) + n_{1,3,2}(x,l,ws_{1,3}(x,l)) + n_{1,3,3}(x,l,ws_{1,3}(x,l)) & i=1, j=3, \frac{k}{4}+2 \le x \le \frac{k}{8}, 1 \le l < \log_2 k - 1 \end{cases} \quad (43)$$

$$F'(L,L_b,L_c) = [f'_1, f'_2, f'_3]$$
$$= \left[\sum_{i=1}^{\log_2 k-2} (L^{2\log_2 k-3-i} L_b^{2B_n[0:\log_2 k-1]-B_n[0:i]} L_c^{W_{\max}[i-1:\log_2 k-1]+W_{\max}[2:\log_2 k-2]}), L^{\log_2 k-2} L_b^{B_n[0:\log_2 k-1]} L_c^{W_{\max}[2:\log_2 k-2]} \right.$$
$$\left. \sum_{i=1}^{\log_2 k-2} (L^{i-1} L_b^{B_n[0:i]} L_c^{W_{\max}[2:i]}) \right] \quad (44)$$

$$N^D_{i,j\,w\text{case}}(x,l,ws_{i,j}(x,l))$$
$$= \begin{cases} P_{\text{in}}(L_{2,0}L_{2,3}L_b^6(X_{p1}L_c^2L_{p0} + L_{c1}X_c) + \frac{L_{3,1}L_{0,2}}{L_c^2}X_c) & i=0, j=2, x=1, l=1 \\ P_{\text{in}}(L_{1,3}L_{3,1}L_{3,2}L_b^7L_c^2\beta_2 + L_{1,3}L_b^5(\frac{L_{2,0}}{L_cL_{c0}}X_c + \frac{L_{3,1}}{L_{c1}}(X_{p1}+L_{p1}X_c))) & i=2, j=0, x=1, l=2 \\ P_{\text{in}}(L_{1,3}L_{3,0}^{l-2}L_{2,1}^{l-3}L_{3,2}L_b^{B_n[0:l+2]}L_c^{W_{\max}[l:l+1]+W_{\max}[l-1:l]}\beta_2), & \\ +P_{\text{in}}(L_{0,2}L_{2,0}^{l-2}L_b^{2l}L_c^{W_{\max}[l-2:l-1]}(\frac{L_{2,0}}{L_cL_{c0}}X_c + \frac{L_{3,1}}{L_{c1}}(X_{p1}+L_{p1}X_c))) & i=2, j=0, 1 < x < \frac{k}{8}, 2 < l < log_2k - 1 \\ P_{\text{in}}(L_{0,2}L_{2,1}^{l-3}L_{3,1}L_{2,0}L_b^{B_n[0:l+1]}L_c^{W_{\max}[l-2:l-1]}\beta_2), & \\ +P_{\text{in}}(L_{0,2}L_{2,0}L_{3,0}^{l-3}L_b^{B_n[0:l]+1}(\frac{L_{2,0}}{L_cL_{c0}}X_c + \frac{L_{3,1}}{L_{c1}}(X_{p1}+L_{p1}X_c))) & i=2, j=0, x=\frac{k}{8}, l=log_2k-1 \end{cases} \quad (45a)$$

$$N^U_{i,j\,w\text{case}}(x,l,ws_{i,j}(x,l))$$
$$= \begin{cases} P_{\text{in}}(L_{0,2}L_{2,0}L_{3,0}^{l-3}L_{1,3}L_b^{B_n[0:l+1]}\beta_1), & \\ +P_{\text{in}}(L_{0,2}L_{2,1}^{l-3}L_{3,1}L_b^{B_n[0:l]+1}L_c^{W_{\max}[l-2:l-1]}(L_{p0}^2X_c + X_{p0})) & i=1, j=3, x=\frac{k}{8}+1, l=log_2k-1 \\ P_{\text{in}}(L_{0,2}L_{2,1}^{l-2}L_{2,0}L_{2,3}L_b^{B_n[0:l+2]}L_c^{W_{\max}[l-1:l+1]}\beta_1), & \\ +P_{\text{in}}(L_{0,2}L_{2,1}^{l-3}L_{3,1}L_b^{B_n[0:l]+1}L_c^{W_{\max}[l-2:l-1]}(L_{p0}^2X_c + X_{p0})) & i=1, j=3, \frac{k}{8} < x \le \frac{k}{4}-3, 4 \le l < log_2k-1 \\ P_{\text{in}}(L_{0,2}L_{2,1}L_{2,0}L_{2,3}L_b^9L_c^8\beta_1 + L_{0,2}L_{2,1}L_b^6(L_{p0}^2X_c + X_{p0})) & i=1, j=3, x=\frac{k}{4}-1, l=3 \\ P_{\text{in}}(L_{1,3}L_{3,0}L_{2,3}L_b^9L_c^3(L_cL_{p0}(X_c + L_c^2X_{p0}) + L_{c0}X_c)) & i=1, j=2, x=\frac{k}{4}, l=2 \\ P_{\text{in}}(L_b\beta_2 + L_b^2(\frac{L_{2,0}}{L_cL_{c0}}X_c + \frac{L_{3,1}}{L_{c1}}(X_{p1}+L_{p1}X_c))) & i=2, j=0, x=\frac{k}{2}-1, l=1 \end{cases} \quad (45b)$$

in (43), shown at the top of the page, while (44), shown at the top of the page, calculates the power loss function associated with the accumulated crosstalk noise on the second longest optical link, $F'(L, L_b, L_c)$.

Considering the worst-case SNR link in Fig. 10, when the optical signal travels downward in the lower subnetwork, the worst-case crosstalk noise added to the worst-case SNR link, $N^D_{i,j\,w\text{case}}$, is calculated in (45a), shown at the top of the page. Furthermore (45b), shown at the top of the page, calculates the worst-case crosstalk noise added to the worst-case SNR link while it is travelling upward in the lower subnetwork, $N^U_{i,j\,w\text{case}}$,

This article has been accepted for inclusion in a future issue of this journal. Content is final as presented, with the exception of pagination.

where

$$\beta_1 = \left(\frac{L_{1,3}L_bL_c^2}{L_{c1}}(X_{p1} + L_{p1}X_c) + \frac{L_{0,2}L_{1,3}}{L_c^2L_bL_{c1}}X_c\right)$$
$$\beta_2 = \left(\frac{L_{0,3}L_{2,0}}{L_bL_{c0}L_{c1}}(X_c + L_c^2X_{p0})\right).$$

REFERENCES

[1] L. Benini and G. De Micheli, "Networks on chip: A new paradigm for systems on chip design," in *Proc. DATE*, 2002, pp. 418–419.

[2] (2013). *International Technology Roadmap for Semiconductors (ITRS)* [Online]. Available: http://www.itrs.net

[3] M. Haurylau, G. Chen, H. Chen, J. Zhang, N. A. Nelson, D. H. Albonesi, *et al.*, "On-chip optical interconnect roadmap: Challenges and critical directions," *IEEE J. Sel. Topics Quantum Electron.*, vol. 12, no. 6, pp. 1699–1705, Nov./Dec. 2006.

[4] R. Ramaswami, K. Sivarajan, and G. Sasaki, *et al.*, *Optical networks: a practical perspective*. San Mateo, CA, USA: Morgan Kaufmann, 2009.

[5] E. Goldstein, L. Eskildsen, and A. F. Elrefaie, "Performance implications of component crosstalk in transparent lightwave networks," *IEEE Photon. Technol. Lett.*, vol. 6, no. 5, pp. 657–660, May 1994.

[6] S. Dods, J. P. R. Lacey, and R. S. Tucker, "Performance of WDM ring and bus networks in the presence of homodyne crosstalk," *J. Lightw. Technol.*, vol. 17, no. 3, pp. 388–396, Mar. 1999.

[7] P. Legg, M. Tur, and I. Andonovic, "Solution paths to limit interferometric noise induced performance degradation in ASK/direct detection lightwave networks," *J. Lightw. Technol.*, vol. 14, no. 9, pp. 1943–1954, 1996.

[8] S. Dods and R. Tucker, "A comparison of the homodyne crosstalk characteristics of optical add-drop multiplexers," *J. Lightw. Technol.*, vol. 19, no. 12, pp. 1829–1838, Dec. 2001.

[9] H. Gu, J. Xu, and Z. Wei "A low-power fat tree-based optical network-on-chip for multiprocessor system-on-chip," in *Proc. DATE*, Apr. 2009, pp. 3–8.

[10] Z. Wang, J. Xu, X. Wu, Y. Ye, W. Zhang, M. Nikdast, *et al.*, "Floorplan optimization of fat-tree based networks-on-chip for chip multiprocessors," *IEEE Trans. Comput.*, accepted for publication.

[11] Y. Xie, M. Nikdast, J. Xu, X. Wu, W. Zhang, Y. Ye, *et al.*, "Formal worst-case analysis of crosstalk noise in mesh-based optical networks-on-chip," *IEEE Trans. Very Large Scale Integr. (VLSI) Syst.*, vol. 21, no. 10, pp. 1823–1836, Oct. 2013.

[12] Y. Zhang, S. Yang, A. E.-J. Lim, L. Guo-Qiang, C. Galland, T. Baehr-Jones, *et al.*, "A CMOS-compatible, low-loss, and low-crosstalk silicon waveguide crossing," *IEEE Photon. Technol. Lett.*, vol. 25, no. 5, pp. 422–425, Mar. 1, 2013.

[13] A. V. Tsarev, "Efficient silicon wire waveguide crossing with negligible loss and crosstalk," *Opt. Exp.*, vol. 19, no. 15, pp. 13732–13737, 2011.

[14] W. Ding, D. Tang, Y. Liu, L. Chen, and X. Sun, "Compact and low crosstalk waveguide crossing using impedance matched metamaterial," *Appl. Phys. Lett.*, vol. 96, no. 11, pp. 111114-1–111114-3, 2010.

[15] F. Xia, L. Sekaric, M. O'Boyle, and Y. Vlasov, "Coupled resonator optical waveguides based on silicon-on-insulator photonic wires," *Appl. Phys. Lett.*, vol. 89, no. 4, pp. 041122-1–041122-3, 2006.

[16] F. Xia, M. Rooks, L. Sekaric, and Y. Vlasov, "Ultra-compact high order ring resonator filters using submicron silicon photonic wires for on-chip optical interconnects," *Opt. Exp.*, vol. 15, no. 19, pp. 11934–11941, 2007.

[17] Q. Li, M. Soltani, S. Yegnanarayanan, and A. Adibi, "Design and demonstration of compact, wide bandwidth coupled-resonator filters on a silicon-on-insulator platform," *Opt. Exp.*, vol. 17, no. 4, pp. 2247–2254, 2009.

[18] Y. Xie, M. Nikdast, J. Xu, W. Zhang, Q. Li, X. Wu, *et al.*, "Crosstalk noise and bit error rate analysis for optical network-on-chip," in *Proc. DAC*, 2010, pp. 657–660.

[19] M. Nikdast, J. Xu, X. Wu, W. Zhang, Y. Ye, X. Wang, *et al.*, "Systematic analysis of crosstalk noise in folded-torus-based optical networks-on-chip," *IEEE Trans. Comput. Aided Des. Integr. Circuits Syst.*, accepted for publication.

[20] J. Chan, G. Hendry, K. Bergman, and L. P. Carloni, "Physical-layer modeling and system-level design of chip-scale photonic interconnection networks," *IEEE Trans. Comput. Aided Des. Integr. Circuits Syst.*, vol. 30, no. 10, pp. 1507–1520, Oct. 2011.

[21] D. Ding, B. Yu, and D. Z. Pan, "GLOW: A global router for low-power thermal-reliable interconnect synthesis using photonic wavelength multiplexing," in *Proc. 17th ASP-DAC*, Feb. 2012, pp. 621–626.

[22] B. C. Lin and C. T. Lea, "Crosstalk analysis for microring based optical interconnection networks," *J. Lightw. Technol.*, vol. 30, no. 15, pp. 2415–2420, Aug. 1, 2012.

[23] C. H. Chen, "Waveguide crossings by use of mutlimode taperedstructures," in *Proc. 21st WOCC*, Apr. 2012, pp. 130–131.

[24] X. Zheng, I. Shubin, G. Li, T. Pinguet, A. Mekis, J. Yao, *et al.*, "A tunable 1×4 silicon CMOS photonic wavelength multiplexer/demultiplexer for dense optical interconnects," *Opt. Exp.*, vol. 18, no. 5, pp. 5151–5160, Mar. 2010.

[25] M. Nikdast and J. Xu. (2013). *Crostalk and Loss Analysis Platform (CLAP)*. [Online]. Available: http://www.ust.hk/∼eexu

[26] F. Xia, L. Sekaric, and Y. Vlasov, "Ultracompact optical buffers on a silicon chip," *Nature Photon.*, vol. 1, pp. 65–71, Jan. 2007.

[27] P. Dong, W. Qian, S. Liao, H. Liang, C.-C. Kung, N.-N. Feng, *et al.*, "Low loss silicon waveguides for application of optical interconnects," in *Proc. IEEE Photon. Soc. Summer Topical Meeting Series*, Jul. 2010, pp. 191–192.

Mahdi Nikdast (S'10) was born in Esfahan, Iran, in 1987. He received the Ph.D. degree in electronic and computer engineering from The Hong Kong University of Science and Technology (HKUST), Hong Kong, in 2013.

He is currently with the Mobile Computing System Laboratory, HKUST, where he is involved in signal-to-noise ratio analyses for optical interconnection networks. He has authored or co-authored more than 30 papers in refereed journals and international conference publications. His current research interests include embedded and computing systems, multiprocessor systems-on-chip, networks-on-chip, and optical interconnection networks.

Dr. Nikdast was a recipient of the Second Best Project Award from the Sixth Annual AMD Technical Forum and Exhibition in 2010.

Jiang Xu (S'02–M'07) received the Ph.D. degree from Princeton University, Princeton, NJ, USA, in 2007.

He is an Associate Professor with the Hong Kong University of Science and Technology, Hong Kong. He is the Founding Director of the Xilinx-HKUST Joint Laboratory and establishes Mobile Computing System Laboratory. He has authored or co-authored of more than 70 book chapters and papers in peer-reviewed journals and international conferences. His current research interests include network-on-chip, multiprocessor system-on-chip, embedded system, computer architecture, low power VLSI design, and hardware/sofware codesign.

Dr. Xu currently serves as an Associate Editor for the *ACM Transactions on Embedded Computing Systems* and the IEEE TRANSACTION ON VERY LARGE SCALE INTEGRATION (VLSI) SYSTEMS. He is an ACM Distinguished Speaker and a Distinguished Visitor of the IEEE Computer Society.

Luan H. K. Duong, photograph and biography not available at the time of publication.

Xiaowen Wu, photograph and biography not available at the time of publication.

Zhehui Wang, photograph and biography not available at the time of publication.

Xuan Wang, photograph and biography not available at the time of publication.

Zhe Wang, photograph and biography not available at the time of publication.